communications physics

ARTICLE

https://doi.org/10.1038/s42005-022-01069-w OPEN

Observation of the proton emitter $^{116}_{57}La_{59}$

Wei Zhang[1✉], Bo Cederwall[1✉], Özge Aktas[1], Xiaoyu Liu[1], Aysegül Ertoprak[1], Ayse Nyberg[1], Kalle Auranen[2], Betool Alayed[3,4], Hussam Badran[2], Helen Boston[3], Maria Doncel[5], Ulrika Forsberg[2], Tuomas Grahn[2], Paul T. Greenlees[2], Song Guo[6], Jacob Heery[2,3], Joshua Hilton[2,3], David Jenkins[7], Rauno Julin[2], Sakari Juutinen[2], Minna Luoma[2], Olavi Neuvonen[2], Joonas Ojala[2], Robert D. Page[3], Janne Pakarinen[2], Jari Partanen[2,9], Edward S. Paul[3], Costel Petrache[8], Panu Rahkila[2], Panu Ruotsalainen[2], Mikael Sandzelius[2], Jan Sarén[2], Stuart Szwec[2], Holly Tann[2,3], Juha Uusitalo[2] & Robert Wadsworth[7]

The quantum tunneling and emission of a single constituent nucleon provide a beautifully simple and unique window into the complex properties of atomic nuclei at the extreme edge of nuclear existence. In particular, for odd-odd proton emitting nuclides, the associated decay energy and partial half-life can be used to probe the correlations between the valence neutrons and protons which have been theoretically predicted to favour a new type of nuclear superfluidity, isoscalar neutron-proton pairing, for which the experimental "smoking gun" remains elusive. In the present work, proton emission from the lanthanum isotope $^{116}_{57}La_{59}$, 23 neutrons away from the only stable isotope $^{139}_{57}La_{82}$, is reported. ^{116}La nuclei were synthesised in the fusion-evaporation reaction ^{58}Ni(^{64}Zn, $p5n$)^{116}La and identified via their proton radioactivity using the mass spectrometer MARA (Mass Analysing Recoil Apparatus) and the silicon detectors placed at its focal plane. Comparisons of the measured proton energy ($E_p = 718 \pm 9$ keV) and half-life ($T_{1/2} = 50 \pm 22$ ms) with values calculated using the Universal Decay Law approach indicate that the proton is emitted with an orbital angular momentum $l = 2$ and that its emission probability is enhanced relative to its closest, less exotic, odd-even lanthanum isotope ($^{117}_{57}La_{60}$) while the proton-emission Q-value is lower. We propose this to be a possible signature for the presence of strong neutron-proton pair correlations in this exotic, neutron deficient system. The observations of γ decays from isomeric states in ^{116}La and ^{117}La are also reported.

[1] Department of Physics, Royal Institute of Technology, Stockholm, Sweden. [2] Department of Physics, University of Jyväskylä, Jyväskylä, Finland. [3] Department of Physics, Oliver Lodge Laboratory, University of Liverpool, Liverpool, UK. [4] Department of Physics, Qassim University, Qassim, Saudi Arabia. [5] Department of Physics, Stockholm University, Stockholm, Sweden. [6] Institute of Modern Physics, Chinese Academy of Sciences, Lanzhou, China. [7] Department of Physics, University of York, York, UK. [8] Université Paris-Saclay, CNRS/IN2P3, IJCLab, Orsay, France. [9] Deceased: Jari Partanen. ✉email: wezh@kth.se; bc@kth.se

Nucleonic pair correlations, also commonly called "pairing", play an important role in the structure of atomic nuclei. Well-known manifestations of the nuclear pairing effect, which is similar to condensed-matter physics phenomena such as superconductivity and superfluidity, are the odd-even staggering of nuclear binding energies[1], seniority symmetry[2–4] in the low-lying spectra of spherical even-even nuclei, and the reduced moments of inertia and backbending effect[5,6] in rotating deformed nuclei. The first fundamental theoretical description of pairing in condensed matter physics focused on the properties of systems composed of large numbers of fermions, such as the electrons in superconductors (Bardeen-Cooper-Schrieffer (BCS) theory[7,8]). The same formalism can be applied to atomic nuclei if the limited number of nucleons that can be bound in such systems is properly taken into account. A basic feature of BCS theory is that it treats systems with identical fermions moving in time-reversed orbitals as correlated pairs with opposite spins ($J = 0$), so-called Cooper pairs. Mean-field models of atomic nuclei based on the BCS approach, such as Hartree–Fock–Bogoliubov theory[9], therefore treat the neutron and proton pairing fields separately. These pairing fields give rise to the nuclear odd-even mass differences for neutrons and protons independently and are called isospin $T = 1$ or isovector pairing. However, the unique coexistence of two distinct fermionic systems (neutrons and protons) in the nucleus may produce additional pairing modes not found elsewhere in Nature. In particular in nuclei with equal or nearly equal neutron and proton numbers ($N \approx Z$) enhanced correlations arise between neutrons and protons that occupy orbitals with the same quantum numbers. The normal isovector pairing mode based on like-particle neutron–neutron (*nn*) and proton–proton (*pp*) Cooper pairs can be generalized to include neutrons and protons which may then also form isospin $T = 1$, angular momentum $J = 0$ *np* pairs and there is evidence for an isovector np condensate in $N \approx Z$ nuclei as would be expected from the isospin invariance of the strong interaction[10]. The long-standing question of the possible presence of a different, isoscalar pairing mode[11–21] predicted to be built from isospin $T = 0$, $J > 0$ *np* pair correlations remains unresolved. Many theoretical calculations predict that isoscalar pairing may only manifest itself clearly in the heaviest, most exotic neutron deficient nuclei with $A > 80$, for a review, see ref. [10]. Calculations using isospin-generalized BCS and HFB equations including *pp*, *nn*, *np* ($T = 1$), and *np* ($T = 0$) Cooper pairs indicated that there may exist a second-order quantum phase transition in the ground states of $N = Z$ nuclei from $T = 1$ pairing below mass 80 to a predominantly $T = 0$ pairing phase above mass 90, with the intermediate mass 80–90 region showing a co-existence of $T = 0$ and $T = 1$ pairing modes[22]. There are even predictions for a dominantly $T = 0$ ground-state pairing condensate in $N \sim Z$ nuclei around mass 130[23].

Proton radioactivity, i.e. spontaneous and direct proton emission, is a rare nuclear decay mode observed for the ground-states or isomeric states of some extremely neutron deficient nuclides (around 30 are known to date). Ground-state proton radioactivity was first observed by Hofmann et al. for ^{151}Lu[24] and by Klepper et al. for ^{147}Tm[25]. The first observation of proton radioactivity in the region of neutron deficient nuclei above tin, was made for ^{109}I and ^{113}Cs by Gillitzer et al.[26]. Proton emission from odd-odd nuclides may reveal effects of the residual proton-neutron interactions between the odd valence neutron and proton[27]. It has previously been observed for a few such cases that the proton-decay Q value, Q_p, of the odd-odd nucleus is lower than that of its less-exotic neighboring odd-even isotope. This was first inferred by Page et al. for the ^{108,109}I pair[28] and recently confirmed by direct measurement of proton emission from ^{108}I by Auranen et al.[29]. Another example is the ^{112,113}Cs pair[30]. Mass models fail consistently in reproducing this behavior. This might be attributed to the attractive residual force between the odd valence neutron and proton in the odd-odd systems[28,31] but the nature of this neutron-proton interaction is until now unknown.

Here, we present the observation of the extremely neutron deficient, $T_Z = 1$, isotope $^{116}_{57}La_{59}$ via its radioactive proton decay and the observation of γ-ray transitions from low-lying microsecond isomers in ^{116,117}La. We propose that the observed differences in measured proton decay Q values and proton formation probabilities between neighboring isotopes provide a new signature and evidence for strong neutron-proton pairing in these exotic systems.

Results

The experiment was performed at the Accelerator Laboratory of the University of Jyväskylä using the ^{58}Ni(^{64}Zn, $p4n$)^{117}La and ^{58}Ni(^{64}Zn, $p5n$)^{116}La fusion-evaporation reactions. Relevant experimental details, in particular regarding the operation of the vacuum-mode recoil separator MARA (Mass Analysing Recoil Apparatus) and the energy calibration of the double-sided silicon strip detector (DSSD) placed at the MARA focla plane, are described in the Methods section of this paper.

Figure 1 shows the decay energy spectra recorded in the DSSD at the beam energy of 330 MeV. The corresponding events were punch-through vetoed and with the requirement that the decay occurred within 100 ms after the implantation of a recoil in the same DSSD quasipixel as well as with the requirement that the multiplicity of evaporated charged particles detected in JYTube (Jyväskylä-York Tube) was 0 or 1. The high background in the low-energy region is mainly from β decays of strongly populated nuclides closer to the stability line. The peak at 808(5) keV corresponds to the proton decay of ^{117}La and its half-life was measured to be $T_{1/2} = 21.6(31)$ ms, in agreement with the previous measurements of the ground-state proton decay of ^{117}La[32–34]. The yield of ~ 680 counts in this peak corresponds to a production cross section of ~ 120 nb, assuming a MARA transmission efficiency of 35% for mass 117.

The low-energy region of the spectrum in Fig. 1 is enlarged and shown in the inset. A small peak at 718(9) keV is clearly visible above the β background with a statistics of 40(14) counts, which we assign to the ground-state proton decay of ^{116}La. These proton-decay events could be further enhanced relative to the β-decay background by requiring that they occurred in delayed coincidence with γ rays at the focal plane of MARA, as explained in Methods. A half-life of $T_{1/2} = 50(22)$ ms was determined for the proton decay of ^{116}La (Methods).

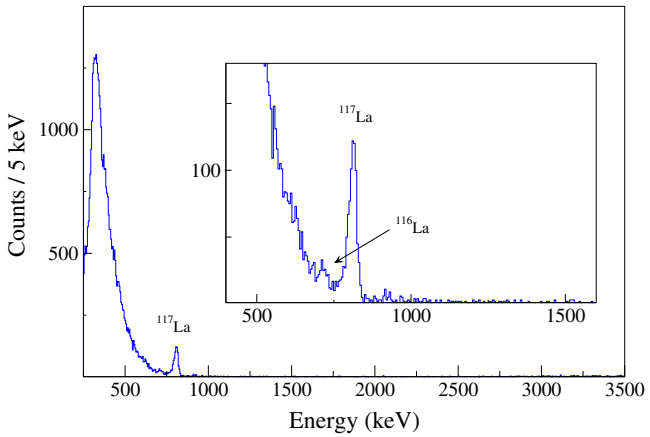

Fig. 1 Energy spectrum of punch-through-vetoed decay events. These events were measured in the DSSD within 100 ms after an ion implantation in the same quasipixel at the beam energy of 330 MeV. The inset shows the enlarged low-energy region. The previously known proton-decay peak of ^{117}La and the newly observed proton-decay peak of ^{116}La are indicated.

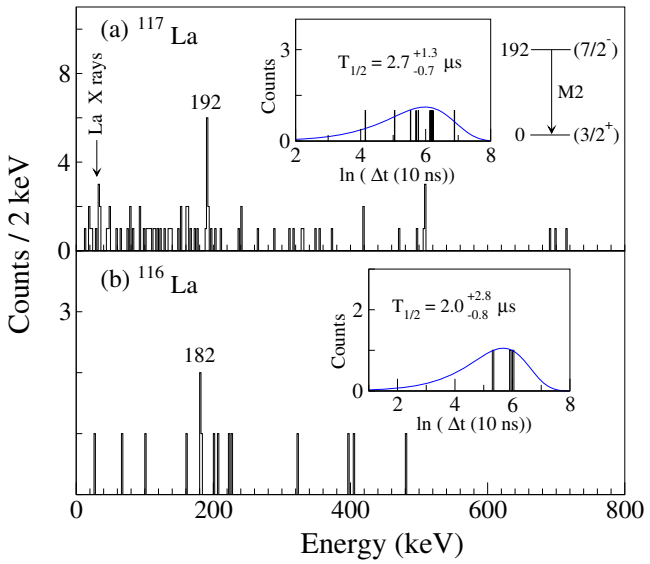

Fig. 2 Experimental data illustrating the two observed isomeric-γ transitions. a γ-ray energies detected within 8 μs of a recoil implantation into the DSSD and followed by a proton decay from ^{117}La in the same quasipixel. The inset shows the time distribution of 192-keV γ-rays selected in this way. The fit of the lifetime using the maximum likelihood method[35] is indicated by the blue curve. The proposed corresponding level scheme obtained for ^{117}La is indicated to the right. **b** Same as **a** tagged by ^{116}La proton decays and for 182-keV γ-rays.

Recoil-γ-decay event chains were investigated in order to search for isomeric γ-ray transitions in ^{117}La and the newly discovered isotope ^{116}La. The γ-ray energy spectrum recorded by the clover high-purity germanium (HPGe) detectors sourrounding the MARA focal plane for events registered within 8 μs of a recoil implantation and gated by ^{117}La protons (Fig. 2a), reveals a peak with 9 counts at 192 keV. Based on a maximum likelihood analysis[35], a lifetime $\tau = 3.9^{+1.9}_{-0.9}\mu$s ($T_{1/2} = 2.7^{+1.3}_{-0.7}\,\mu$s) was determined for the corresponding isomeric level. Using Weisskopf estimates, we assign the multipolarity of the 192 keV transition to be of magnetic quadrupole (M2) character (see Methods for details). A tentative spin-parity $7/2^-$ is consequently assigned to the 192 keV level, based on the previous assignment of the ground state as $(3/2^+)$[32,34]. The intensity of the observed 192 keV transition indicates an isomeric population ratio of the order of 30%. This would be in agreement with the observation of prompt γ rays from ^{117}La by Liu et al.[34] if a significant fraction of those γ rays emanate from a rotational cascade feeding the isomer. Evidence for an isomeric M2 transition at an energy of 182 keV was also observed to be correlated with the proton decay of ^{116}La, as shown in Fig. 2b. Its half-life was determined to be $T_{1/2} = 2.0^{+2.8}_{-0.8}\mu$s.

Discussion

The ground-state and low-lying yrast configurations of the neutron deficient lanthanum isotopes are predicted to be moderately quadrupole-deformed ($\beta_2 \approx 0.3$)[36] and based on valence protons occupying Nilsson[37] orbits from the near-degenerate $2d_{5/2}$ and $1g_{7/2}$ sub-shells. Levels based on configurations with $g_{9/2}/h_{11/2}$ spherical parentage that extrude/intrude with increasing deformation may also come close to the Fermi level. The detailed balance determining which configuration actually forms the ground state may provide important input for stringent tests of effective nucleon-nucleon interactions used in current nuclear models. This situation also provides the necessary requirements for nuclear isomerism created by yrast spin traps[38,39]. The relevant Nilsson configurations near the Fermi level have been discussed extensively in the literature for neighboring isotopes closer to the line of beta stability, see e.g. the recent work on ^{119}Cs[40]. In ^{121}La, the most neutron deficient lanthanum isotope for which excited states have been reported prior to this work, two rotational bands have been observed and assigned to be built on the $9/2^+[404]$ and $1/2^-[550]$ Nilsson orbitals[41].

In theoretical studies of the proton emission rate from ^{117}La the adiabatic approach[42] suggested ground-state spin-parity $J^\pi = 3/2^+$[32], while non-adiabatic calculations[43,44] proposed $J^\pi = 3/2^+$ or $J^\pi = 3/2^-$. The $J^\pi = 3/2^+$ assignment corresponds to the $3/2^+[422]$ Nilsson orbital[40] of mainly $2d_{5/2}$ parentage and hence emission of predominantly $l = 2\hbar$ protons. On the other hand, $J^\pi = 3/2^-$ would correspond to the $3/2^-[541]$ $1h_{11/2}$ intruder configuration[40] and, consequently, $l = 5\hbar$ proton emission which would be expected to be subject to additional strong hindrance due to the larger centrifugal barrier. For the proton emitter ^{121}Pr, it was proposed[45] that the $J^\pi = 7/2^-$ member of such a configuration could form the ground state as a result of a strong Coriolis interaction, i.e. a kinematic coupling of the angular momenta of the odd valence proton and the core. Even if this state is unlikely to form the ground state of ^{117}La it may well produce a low-lying excited state resulting in a spin-trap isomer. The 192-keV M2 transition found in this work is therefore assigned to populate the $3/2^+$ ground state from this $7/2^-$ state as indicated in Fig. 2. For ^{116}La, the spin-parity of its ground-state is considerably more difficult to assess due to the numerous possibilities to couple the low-lying proton and neutron configurations. Therefore, even though the 182-keV M2 isomeric transition is most likely of similar character, it was not placed into a tentative level scheme.

The Universal Decay Law is a convenient, model independent microscopic approach to quantum tunneling theory which can be applied to all forms of ground-state to ground-state radioactive decays involving the emission of protons and heavier charged particles[46,47]. The half-life can be expressed as[42,46]

$$T_{1/2} = \frac{\hbar \ln 2}{\Gamma_l} = \frac{\ln 2}{v} \left| \frac{H_l^+(\chi,\rho)}{RF_l(R)} \right|^2 \quad (1)$$

where l is the angular momentum carried by the emitted particle and v is its outgoing velocity. In the case of proton emission, the distance parameter, R, denotes the point where the radial wave function describing the proton in the internal region of the nucleus is matched with its outgoing wave function. H_l^+ is the Coulomb-Hankel function which can be well approximated by the Wentzel–Kramers–Brillouin (WKB) value[48]. The "formation probability", $|RF_l(R)|^2$, which should not be confused with the probability to form a complex cluster such as an α particle inside the nucleus, is similar to the spectroscopic factor commonly deduced from proton decay observables and can be extracted from Eq. (1). It provides a more precise evaluation of the influence of the nuclear structure on the proton decay width, especially in the case of a deformed nucleus[47].

Figure 3 and Table 1 show the $|RF_l(R)|^2$ values as extracted from the experimental half-lives and Q values from the ground-state proton-decays observed to date in odd-Z elements between $Z = 53$ and 83[29,49–51]. In the present analysis it was not possible to accurately measure the β-decay branching ratio for the ground-state decay of ^{116}La. Based on the theoretical calculations by Möller et al., which predicted a partial β-decay half-life of 124 ms for ^{116}La[52], the proton-decay branching ratio is estimated to be 60(18)% and, consequently, the partial proton-decay half-life is deduced as $T_{1/2,p} = 84^{+86}_{-50}$ ms. The formation probability for ^{116}La is furthermore calculated under two alternative assumptions; that the orbital angular momentum carried by the emitted proton is $l_p = 2\hbar$

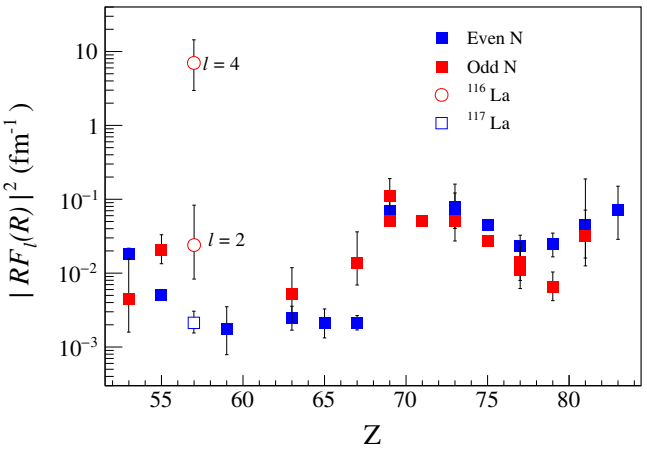

Fig. 3 Proton formation probabilities. These formation probabilities, $|RF_l(R)|^2$, were deduced for the ground-state proton decays in the odd-Z elements between $Z = 53$ and 83 as a function of the proton number Z. Experimental uncertainties in the half-lives and Q-values have been taken into account in the error bars. The formation probability for ^{117}La has been calculated using the proton orbital angular momentum $l_p = 2\hbar$ and for ^{116}La using two alternative values, $l_p = 2\hbar$ and $l_p = 4\hbar$. Detailed information on the values of l_p, Q_p and half-lives used for the calculation as well as the derived formation probabilities for all displayed proton-emitters are summarized in Table 1.

or $l_p = 4\hbar$. Analogous to the proton decay of ^{117}La[34], it is reasonable to assume that the proton component of the ground-state wave function of ^{116}La is predominantly of $d_{5/2}$ parentage.

It can be observed that the proton formation probabilities shown in Fig. 3, are divided into two main regions at $Z = 69$, where $|RF_l(R)|^2$ reaches the maximum value for the nucleus $^{144}_{69}$Tm. Focusing first on the even-N nuclides in the region with $Z \geq 69$ they have consistently the largest $|RF_l(R)|^2$ values with a dip appearing around $_{77}$Ir - $_{79}$Au. The behavior is associated with the nuclear deformation of these proton emitters which are predicted to be spherical or weakly-deformed in this region[36] and the ground-state proton wave function to be dominated by a single-particle orbit[53,54]. Consequently, the formation probability of this region is generally large, and the dip in $|RF_l(R)|^2$ around the iridium and gold proton emitters is likely related to the transitional onset of weakly-deformed shapes[36]. For the proton emitters with $Z < 69$ the $|RF_l(R)|^2$ values are consistently around one order of magnitude smaller and it was noted that this may be expected in this deformed region[48] for which the decay primarily involves only the low- l components of the deformed ground-state configuration[42,54,55]. However, the deformation effect on the formation probability seems to saturate already at moderate deformations since the $|RF_l(R)|^2$ values exhibit a nearly constant trend also beyond the strongly deformed $_{63}$Eu - $_{67}$Ho rare-earth nuclei. For the weakly deformed $_{53}$I - $_{55}$Cs nuclei the $|RF_l(R)|^2$ values again start increasing as a function of decreasing Z, approaching the spherical shapes close to the doubly-magic, self-conjugate nucleus $^{100}_{50}$Sn$_{50}$.

Turning now to the odd-odd isotopes, the differences between the ground-state to ground-state proton-decay Q values of the odd-N proton-emitters and their less exotic nearest even-N isotopes, $\Delta Q_p^{oe} = Q_p^N - Q_p^{N+1}$ (N odd), are known to be negative only for four pairs; $\Delta Q_p^{oe} = -222(14)$ keV for $^{108,109}_{53}$I[29], $\Delta Q_p^{oe} = -153(8)$ keV for $^{112,113}_{55}$Cs[30], $-91(10)$ keV for $^{116,117}_{57}$La, and $-84(11)$ keV for $^{140,141}_{67}$Ho[56]. The reduced Q_p values for the odd-odd proton-emitters reflect that the valence proton is more strongly bound. It was first noticed by Page et al.[28,30] for the isotopic pairs $^{108,109}_{53}$I and $^{112,113}_{55}$Cs, and attributed to "strong pairing forces" between the odd valence neutron and proton. Modern nuclear mass models, such as FRDM[36] and KTUY05[57], fail to predict decreasing Q_p values when moving away from stability.

A striking effect is visible in Fig. 3, namely that three of the odd-N isotopes in the deformed region; $^{112}_{55}$Cs, $^{116}_{57}$La, and $^{140}_{67}$Ho have significantly larger $|RF_l(R)|^2$ values than the closest, less exotic, even-N isotope around an order of magnitude, while for $^{108,109}_{53}$I the difference between the corresponding $|RF_l(R)|^2$ values is within the experimental uncertainties and therefore inconclusive. This implies that in these odd-odd nuclei ^{112}Cs, ^{116}La, and ^{140}Ho, the presence of the odd valence neutron induces a facilitating effect on the proton emission compared with the neighboring isotope where all neutrons are paired. The enhanced $|RF_l(R)|^2$ values for these odd-odd proton emitters and the corresonding negative ΔQ_p^{oe} values for $^{112,113}_{55}$Cs, $^{116,117}_{57}$La, and $^{140,141}_{67}$Ho isotopic pairs stand out by themselves. The *coincidence* of these quantities is even more remarkable and seems to require an explanation beyond the current understanding of proton radioactivity.

We have considered various mechanisms that might explain the observed effect and find that a plausible scenario involves neutron-proton pairing, which may be enhanced in extremely neutron deficient nuclei for which neutron and proton numbers are approximately equal and neutrons and protons near the Fermi level therefore move in similar orbits. The properties of odd-odd nuclides are of particular interest in this sense since like-particle pair correlations are expected to be blocked by the odd valence particles.

How could then an enhanced *np* pairing strength contribute simultaneously to the increased binding and increased proton emission probability in some deformed odd-odd proton emitters? While evidence for the the presence of *isoscalar* pair correlations remains rather elusive and has only been found in a few of the heaviest nuclei at the $N = Z$ line[18–21], there is more ubiquitous evidence that *np* pairing of the *isovector* type may coexist with the like-particle pairing fields[10]. In particular, it has been shown that the binding energy differences between even-even and odd-odd $N = Z$ nuclei are likely to be associated with isovector pairing[58]. However, the enhancement of the $|RF_l(R)|^2$ values and spectroscopic factors (see Table 1) for the odd-odd proton emitters, which indicate that the odd neutron facilitates the emission of the proton, seems at first glance contradictory to a situation with an increased binding of the same. On the other hand, for a large *np* pair gap of the isovector type one may expect properties similar to "normal" isovector pairing of the like-particle type[10]. Such pair correlations have commonly been assumed to become especially important at the nuclear surface, but there are few rigorous treatments of this difficult problem. Pastore et al.[59] investigated the spatial distribution of the pairing density in ^{120}Sn using a bare nucleon-nucleon potential approach as well as with a pairing interaction induced by the exchange of collective vibrations. The resulting pairing density was found to be strongly peaked on the nuclear surface. This study included only the neutron degrees of freedom in the pairing field, i.e. nucleon pairs carrying isospin $T = 1$ excitations.

We propose that a mechanism by which the odd proton in an odd-odd nucleus experiences stronger binding while at the same time the proton emission probability is enhanced could be via an isovector *np* pairing field. In $N \approx Z$ nuclei, isovector *np* pairs are likely to coexist with like-particle *nn* and *pp* pairs [10]. As a natural consequence of the charge independence of the strong interaction, isovector *np* pairing should have the same features as normal, isovector pairing. Following the results of Pastore et al., an enhanced isovector *np* pairing density at the nuclear surface would then result in a more surface-peaked proton density

Table 1 Calculated proton formation probabilities and spectroscopic factors for the ground-state proton emitters.

Emitter	l_p	Q_p (keV)	$T^p_{1/2}$(exp)	$\|RF_l(R)\|^2(fm^{-1})$	Orbit	$T^{th}_{1/2}$(WKB)	S_{exp} (%)
$^{108}_{53}$I	2	605(13)	5.3(2.2) s	$0.004^{+0.011}_{-0.003}$	$2d_{5/2}$	89^{+95}_{-45} ms	$1.7^{+4.2}_{-1.1}$
$^{109}_{53}$I	2	827(5)	93.5(5) μs	0.018(3)	$2d_{5/2}$	6.2(11) μs	6.6(12)
$^{112}_{55}$Cs	2	823(7)	0.5(1) ms	$0.021^{+0.012}_{-0.008}$	$2d_{5/2}$	41^{+12}_{-9} μs	8^{+5}_{-3}
$^{113}_{55}$Cs	2	976(3)	16.7(7) μs	0.005(1)	$2d_{5/2}$	0.33(3) μs	2.0(3)
$^{116}_{57}$La	2	734(9)	84^{+86}_{-50} ms	$0.023^{+0.06}_{-0.015}$	$2d_{5/2}$	$8.6^{+4.2}_{-2.6}$ ms	10^{+28}_{-6}
$^{117}_{57}$La	2	825(5)	23.1(3.6) ms	$0.0021^{+0.0009}_{-0.0006}$	$2d_{5/2}$	$0.21^{+0.05}_{-0.03}$ ms	$0.9^{+0.4}_{-0.3}$
$^{121}_{59}$Pr	2	900(10)	10^{+6}_{-3} ms	$0.0018^{+0.0017}_{-0.001}$	$2d_{5/2}$	84^{+33}_{-24} μs	$0.8^{+0.8}_{-0.5}$
$^{130}_{63}$Eu	2	1039(15)	$0.90^{+0.49}_{-0.29}$ ms	$0.005^{+0.007}_{-0.003}$	$2d_{5/2}$	26^{+14}_{-9} μs	3^{+4}_{-2}
$^{131}_{63}$Eu	2	959(9)	$21.4^{+1.8}_{-1.7}$ ms	$0.0025^{+0.0011}_{-0.0008}$	$2d_{5/2}$	0.3(1) ms	$1.4^{+0.6}_{-0.5}$
$^{135}_{65}$Tb	3	1200(7)	$0.94^{+0.33}_{-0.22}$ ms	$0.0021^{+0.0012}_{-0.0008}$	$1h_{11/2}$	7.6(14) ms	> 100
$^{140}_{67}$Ho	3	1106(10)	6(3) ms	$0.014^{+0.022}_{-0.007}$	$1h_{11/2}$	320^{+110}_{-80} ms	> 100
$^{141}_{67}$Ho	3	1190(8)	4.1(1) ms	$0.0021^{+0.0006}_{-0.0004}$	$1h_{11/2}$	32(7) ms	> 100
$^{144}_{69}$Tm	5	1725(16)	$2.7^{+1.7}_{-0.7}$ μs	$0.11^{+0.08}_{-0.06}$	$1h_{11/2}$	$2.9^{+0.8}_{-0.6}$ μs	~ 100
$^{145}_{69}$Tm	5	1753(7)	3.46(32) μs	$0.056^{+0.012}_{-0.01}$	$1h_{11/2}$	1.8(2) μs	53(11)
$^{146}_{69}$Tm	5	1210(4)	117.6(64) ms	$0.051^{+0.009}_{-0.007}$	$1h_{11/2}$	67(7) ms	57^{+10}_{-8}
$^{147}_{69}$Tm	5	1073(5)	3.78(1.27) s	$0.069^{+0.052}_{-0.025}$	$1h_{11/2}$	3.0(5) s	80^{+60}_{-30}
$^{150}_{71}$Lu	5	1283(3)	64.0(56) ms	0.05(1)	$1h_{11/2}$	38(3) ms	60(10)
$^{151}_{71}$Lu	5	1253(3)	127.1(18) ms	0.051(5)	$1h_{11/2}$	77(6) ms	61(6)
$^{155}_{73}$Ta	5	1468(15)	$2.9^{+1.5}_{-1.1}$ ms	$0.056^{+0.065}_{-0.029}$	$1h_{11/2}$	$2.0^{+0.7}_{-0.5}$ ms	69^{+82}_{-36}
$^{156}_{73}$Ta	2	1032(5)	149(8) ms	$0.05^{+0.013}_{-0.01}$	$2d_{3/2}$	70^{+13}_{-11} ms	47^{+12}_{-9}
$^{157}_{73}$Ta	0	947(7)	300(105) ms	$0.08^{+0.08}_{-0.035}$	$3s_{1/2}$	170(50) ms	56^{+56}_{-25}
$^{160}_{75}$Re	2	1287(6)	687(11) μs	0.027(5)	$2d_{3/2}$	0.18(3) ms	26(5)
$^{161}_{75}$Re	0	1214(6)	0.440(2) ms	0.045(7)	$3s_{1/2}$	0.14(3) ms	32(6)
$^{164}_{77}$Ir	5	1844(9)	113^{+62}_{-30} μs	$0.014^{+0.008}_{-0.006}$	$1h_{11/2}$	$21.5^{+3.2}_{-2.8}$ μs	20(10)
$^{166}_{77}$Ir	2	1168(7)	152(71) ms	$0.011^{+0.015}_{-0.005}$	$2d_{3/2}$	18(4) ms	12^{+15}_{-6}
$^{167}_{77}$Ir	0	1096(6)	110(15) ms	$0.023^{+0.01}_{-0.006}$	$3s_{1/2}$	20^{+5}_{-4} ms	18^{+8}_{-5}
$^{170}_{79}$Au	2	1488(12)	321^{+67}_{-58} μs	0.007(3)	$2d_{3/2}$	23(6) μs	7^{+4}_{-3}
$^{171}_{79}$Au	0	1464(10)	$24.5^{+4.7}_{-3.1}$ $m\mu$s	$0.025^{+0.01}_{-0.008}$	$3s_{1/2}$	$4.9^{+1.2}_{-1}$ μs	20^{+8}_{-6}
$^{176}_{81}$Tl	0	1282(18)	$5.2^{+3.0}_{-1.4}$ ms	$0.032^{+0.039}_{-0.019}$	$3s_{1/2}$	$1.5^{+1.0}_{-0.6}$ ms	29^{+35}_{-18}
$^{177}_{81}$Tl	0	1180(20)	67(37) ms	$0.05^{+0.14}_{-0.03}$	$3s_{1/2}$	28^{+24}_{-13} ms	41^{+130}_{-26}
$^{185}_{83}$Bi	0	1624(16)	$3.0^{+2.5}_{-1.1}$ μs	$0.07^{+0.08}_{-0.03}$	$3s_{1/2}$	2.0(7) μs	64^{+72}_{-38}

The experimental Q_p values (including the recoil and electron screening corrections[68]), the partial proton emission half-lives, $T^p_{1/2}$, and the emitted angular momentum l_p (used for the formation probability calculation), as well as the specified spherical orbitals (for the calculation of half-lives, $T^{th}_{1/2}$) are taken from refs. [29,49–51], apart from the results for ^{116,117}La obtained in the present work. The theoretical half-lives, $T^{th}_{1/2}$, are calculated within the WKB approximation using the Becchetti-Greenless optical model parameters[69] and the experimental spectroscopic factors are determined as ratios of calculated and measured half-lives, $S_{exp} = T^{th}_{1/2}/T^p_{1/2}$. For the odd-odd proton emitters, it is assumed that the valence neutron remains the same configuration in the parent and daughter nuclei. Experimental uncertainties in the half-lives and Q-values have been taken into account when calculating the error bars of the formation probabilities and spectroscopic factors.

distribution, thereby facilitating the tunneling process through the Coulomb and centrifugal barriers. A dynamic enhancement of the proton emission probability involving *np* pairs scattering into proton continuum states could also play a role in such a process. The fact that the effect is not observed in the region of near-spherical or weakly deformed nuclei is consistent with a smaller pairing gap in these nuclei while the deformed region with its higher level density and larger pairing gap, as well as closer proximity to the $N = Z$ line seems more favorable. The absence of a sizeable effect for the $^{130,131}_{63}$Eu pair is then readily explained as a result of the neutron and proton Fermi levels being situated in single-particle orbitals emanating from different major oscillator shells[60], thereby reducing neutron-proton correlations.

Whether the observed effect could also be explained by *np* pairing of the *isoscalar* type is a possibility that requires theoretical model development beyond the current state of the art. These observations highlight the importance of proton emission as a probe of fundamental nuclear structure and illustrate the need for pushing the experimental boundaries of proton emission measurements further.

Conclusions

The extremely neutron deficient isotope ^{116}La has been observed via its ground-state proton emission ($E_p = 718(9)$ keV, $T_{1/2} = 50(22)$ ms). The proton decay of ^{117}La has also been remeasured ($E_p = 808(5)$ keV, $T_{1/2} = 21.6(31)$ ms). Isomeric transitions of M2 character belonging to ^{117}La and ^{116}La were observed with energies and corresponding half-lives ($E_\gamma = 192$ keV, $T_{1/2} = 2.7^{+1.3}_{-0.7}$ μs) and ($E_\gamma = 182$ keV, $T_{1/2} = 2.0^{+2.8}_{-0.8}$ μs), respectively. An enhanced proton emission probability for ^{116}La as well as for a few other odd-odd proton emitters compared with their neighboring, less-exotic, odd-even isotopes is observed and found to coincide with negative ΔQ^{oe}_p values in the same cases. This unexpected effect is proposed as a possible manifestation of strong neutron-proton pairing of the isovector type in these systems.

Methods

Experimental details. The ^{64}Zn beam was accelerated by the K130 cyclotron and used to impinge upon an isotopically enriched (99.8%) metallic target foil of ^{58}Ni with an areal density of 750 μg cm^{-2}. During the main production run (39 h of irradiation time) the beam kinetic energy was 330 MeV with an average intensity of 4.8 pnA. The charged-particle detector array JYTube[61] was arranged at the target position to detect evaporated charged particles emitted in the reactions. The fusion residues recoiled out of the target, and were transmitted and separated according to their mass to electric charge state ratio, A/q, to the focal plane detector system of the vacuum-mode recoil separator MARA[62]. The electric and magnetic dipole fields of MARA were set to accept fusion residues with mass $A = 117$ and (nominally) charge state $q = 30.5^+$ for the central "reference" trajectory and to accept recoils in four charge states from 29^+ to 32^+. At the MARA focal plane, recoils were passed through a position-sensitive multiwire proportional counter before being implanted into a DSSD[61,62]. The DSSD was 300 μm thick, with an active area

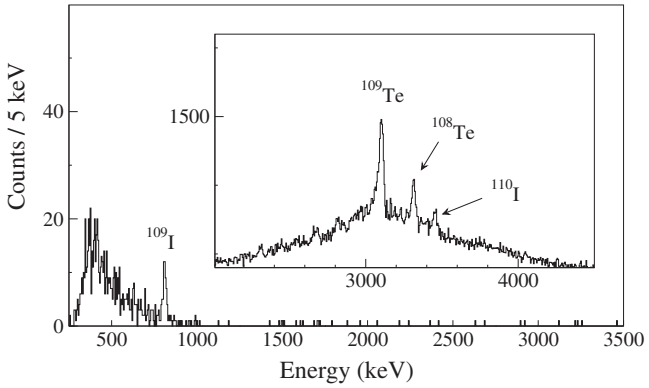

Fig. 4 Energy spectrum of punch-through-vetoed decay events. These events were measured in the DSSD within 300 μs of an ion implantation into the same quasipixel at the beam energy of 370 MeV. The proton-decay peak of ^{109}I is indicated. The inset shows α-decay peaks from ground-state decays of ^{110}I and ^{108,109}Te obtained by applying a recoil-decay correlation time of 3 s.

of 128 mm × 48 mm, and was electrically segmented into 72 vertical strips in the y plane and 192 horizontal strips in the x plane, giving a total of 13824 quasipixels. A second layer of silicon with a thickness of 500 μm was located directly behind the DSSD to veto punch-through events due to uncorrelated high-energy light charged particles and to detect β particles escaping after leaving a partial energy signal in the DSSD. Five clover HPGe detectors were placed surrounding the focal plane of MARA in a close-packed geometry and used for the measurement of delayed γ rays following recoil implantations and/or charged particle decays detected in the DSSD. All detector signals were time stamped using a global 100 MHz clock and recorded independently by the triggerless data acquisition system[63]. The data were analyzed online and offline using the GRAIN software package[64].

The energy calibration of the DSSD was accomplished using a standard mixed-isotope (^{241}Am, ^{244}Cm, ^{239}Pu) α radioactive source with its three main α-energy peaks, as well as in-beam data for the known proton decay of ^{109}I[50], its α-decaying daughter ^{108}Te, and the α-emitters ^{109}Te and ^{110}I[65]. The ^{109,110}I and ^{108,109}Te ions were produced in reactions using a higher beam energy of 370 MeV in a brief run after the main experiment, see the corresponding characteristic proton and alpha decay peaks in Fig. 4.

Weisskopf estimates. The single-particle estimates provide a reasonable relative comparison of electromagnetic transition rates and allow ones to make some general predictions about which multipole is most likely to be emitted[66]. The estimates for mean lifetimes used in this work are as follows

$$\begin{aligned}\tau(\mathrm{M2}) &= \frac{1}{3.5\times 10^7 A^{2/3}E_\gamma^5}\ \mathrm{s}\\ \tau(\mathrm{E3}) &= \frac{1}{3.39\times 10^1 A^2 E_\gamma^7}\ \mathrm{s}\\ \tau(\mathrm{E2}) &= \frac{1}{7.28\times 10^7 A^{4/3}E_\gamma^5}\ \mathrm{s}\end{aligned} \quad (2)$$

where A is the mass number and E_γ is the energy of the γ-ray in MeV. For the new observed 192-keV isomeric-γ ray for ^{117}La, the estimated lifetime of an M2 transition is 4.6 μs which is in fair agreement with the measured lifetime $3.9^{+1.9}_{-0.9}$μs. In contrast, the lifetime for a state depopulated entirely by an E3 transition of the same energy would be 0.22 s, while the estimated lifetime of an E2 transition would be 0.09 μs (equivalent to about one fifth of the flight time through the MARA separator). The isomeric state is most likely situated at 192 keV excitation energy since there are no significant other peaks present in the spectrum of Fig. 2a, apart from La X-rays which are expected due to internal conversion of the M2 transition.

Mass and half-life determinations for the proton decay of ^{116}La. Figure 5a displays the energy spectrum for decay events occurring within 100 ms of a recoil implantation in the DSSD and in delayed coincidence with recoil-decay-correlated isomeric γ rays. In this way, the dominant β background in the DSSD spectra could be greatly reduced and the new proton peak assigned to ^{116}La becomes more pronounced. The inset shows a two-dimensional spectrum of decay energy versus ion mass number, where only ions with charge state 29^+ were selected. For this charge state the recoil implantation rate was substantially lower with a correspondingly lower burden of random correlations between the implantation of fusion residues and β rays. The upper part of the inset to Fig. 5a shows the measured mass distributions for recoils with mass 116 and 117 in the same charge state. The distributions drawn in red and blue correspond to the strongly populated nuclides ^{116}I and ^{117}Xe, respectively, which are obtained by gating on their

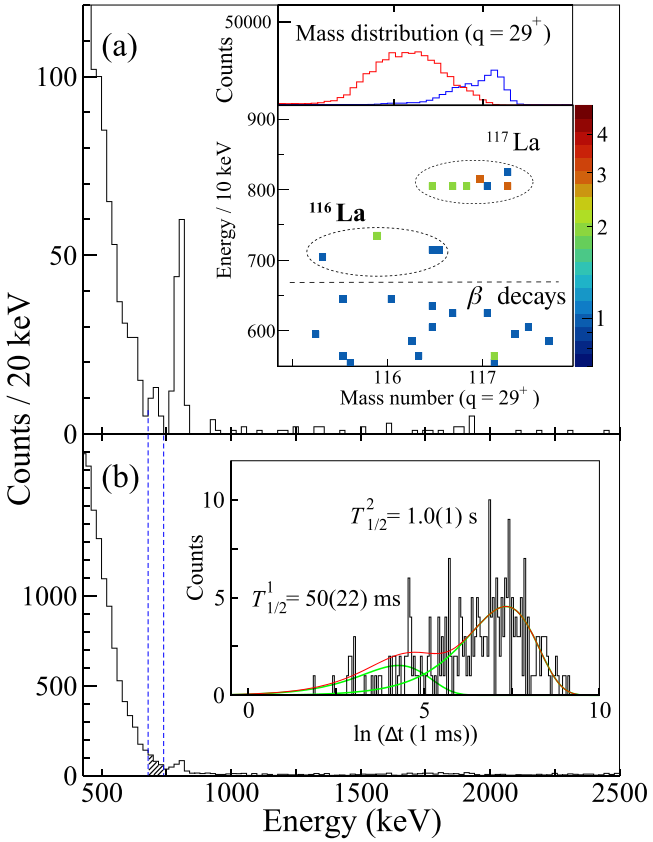

Fig. 5 Experimental data illustrating the observed proton decay of ^{116}La. The decay events measured in the DSSD were in correlation with a prior detection of a recoil-γ event. **a** These decay events were required to occur within 100 ms after recoil implantation into the same DSSD quasipixel. The lower inset shows the two-dimensional distribution of ion mass vs decay energy for ions in charge state $q = 29^+$. The upper inset shows the mass distributions of ^{116}I and ^{117}Xe ions from the same experiment measured in MARA drawn in red and blue, respectively. **b** These decay events were measured within 10 s of a recoil implantation. The blue dashed lines are drawn to illustrate the location of the proton peak of ^{116}La, as indicated by the shaded area. The inset shows the logarithmic time spectrum of the decay events in the shaded region, fitted using a two-component function (red). The green curves show each fitted component. The distribution of higher ln(Δt) values corresponds to the random-correlated β-ray background with its effective fitted half-life.

characteristic isomeric γ rays. In the two-dimensional histogram of energy vs mass the high-energy group corresponds to the ground-state proton decays of ^{117}La, while the low-energy distribution corresponds to β-decay events. The five events in the middle group coincide with the distribution for ions with mass 116 and with the proton line of the new isotope ^{116}La. **b** shows decays within 10 s of a recoil implantation. Using the logarithmic binning method described by Schmidt et al.[35,67], a two-component function was used to fit the lifetime of the decay events within the shaded region of Fig. 5b. This function is given by

$$\left|\frac{dn}{d\theta}\right| = \left(n_1\lambda_1 e^{-\lambda_1 e^\theta} + n_2\lambda_2 e^{-\lambda_2 e^\theta}\right)e^\theta. \quad (3)$$

where $\theta = ln(\Delta t)$ and Δt is the correlation time between decay and recoil and in the unit of ms, n_i and λ_i are the number of counts and decay constants corresponding to the true and random-correlated distributions as shown in the inset of Fig. 5b.

Data availability

Raw data were obtained at the Accelerator Laboratory, University of Jyväskylä, Finland. All other derived data used to support the findings of this study are available from the corresponding authors upon request.

Received: 5 July 2022; Accepted: 31 October 2022;
Published online: 14 November 2022

References

1. Heisenberg, W. Über den bau der atomkerne. *Z. Phys.* **78**, 156–164 (1932).
2. De Shalit, A. & Talmi, I. *Nuclear Shell Theory* (Academic Press, New York, 1963).
3. Talmi, I. *Simple Models of Complex Nuclei*. (Harwood Academic Press, Switzerland, 1993).
4. Rowe, D. & Rosensteel, G. Partially Solvable Pair-coupling models with seniority-conserving interactions. *Phys. Rev. Lett.* **87**, 172501 (2001).
5. Johnson, A., Ryde, H. & Sztarkier, J. Evidence for a "singularity" in the nuclear rotational band structure. *Phys. Lett. B* **34**, 605–608 (1971).
6. Stephens, F. & Simon, R. Coriolis effects in the yrast states. *Nucl. Phys. A* **183**, 257–284 (1972).
7. Bardeen, J., Cooper, L. N. & Schrieffer, J. R. Microscopic theory of superconductivity. *Phys. Rev.* **106**, 162 (1957).
8. Bardeen, J., Cooper, L. N. & Schrieffer, J. R. Theory of superconductivity. *Phys. Rev.* **108**, 1175 (1957).
9. Dobaczewski, J., Flocard, H. & Treiner, J. Hartree-Fock-Bogoliubov description of nuclei near the neutron-drip line. *Nucl. Phys. A* **422**, 103–139 (1984).
10. Frauendorf, S. & Macchiavelli, A. O. Overview of neutron-proton pairing. *Prog. Part. Nucl. Phys.* **78**, 24–90 (2014).
11. Engel, J., Langanke, K. & Vogel, P. Pairing and isospin symmetry in proton-rich nuclei. *Phys. Lett. B* **389**, 211–216 (1996).
12. Engel, J., Pittel, S., Stoitsov, M., Vogel, P. & Dukelsky, J. Neutron-proton correlations in an exactly solvable model. *Phys. Rev. C* **55**, 1781 (1997).
13. Civitarese, O., Reboiro, M. & Vogel, P. Neutron-proton pairing in the BCS approach. *Phys. Rev. C* **56**, 1840 (1997).
14. Goodman, A. L. Hartree-Fock-Bogoliubov theory with applications to nuclei. *Adv. Nucl. Phys.* **11**, 263 (1979).
15. Satuła, W. & Wyss, R. Microscopic structure of fundamental excitations in N = Z nuclei. *Phys. Rev. Lett.* **87**, 052504 (2001).
16. Martínez-Pinedo, G., Langanke, K. & Vogel, P. Competition of isoscalar and isovector proton-neutron pairing in nuclei. *Nucl. Phys. A* **651**, 379–393 (1999).
17. Warner, D. D., Bentley, M. A. & Van Isacker, P. The role of isospin symmetry in collective nuclear structure. *Nat. Phys.* **2**, 311–318 (2006).
18. Cederwall, B. et al. Evidence for a spin-aligned neutron-proton paired phase from the level structure of ^{92}Pd. *Nature* **469**, 68–71 (2011).
19. Cederwall, B. et al. Isospin properties of nuclear pair correlations from the level structure of the self-conjugate nucleus ^{88}Ru. *Phys. Rev. Lett.* **124**, 062501 (2020).
20. Llewellyn, R. D. O. et al. Establishing the maximum collectivity in highly deformed N= Z nuclei. *Phys. Rev. Lett.* **124**, 152501 (2020).
21. Liu, X. et al. Evidence for enhanced neutron-proton correlations from the level structure of the N=Z+1 nucleus $^{87}_{43}Tc_{44}$. *Phys. Rev. C* **104**, L021302 (2021).
22. Goodman, A. L. Proton-neutron pairing in Z = N nuclei with A = 76-96. *Phys. Rev. C* **60**, 014311 (1999).
23. Gezerlis, A., Bertsch, G. F. & Luo, Y. L. Mixed-Spin Pairing condensates in heavy nuclei. *Phys. Rev. Lett.* **106**, 252502 (2011).
24. Hofmann, S. et al. Proton radioactivity of ^{151}Lu. *Z. Phys. A* **305**, 111–123 (1982).
25. Klepper, O. et al. Direct and beta-delayed proton decay of very neutron-deficient rare-earth isotopes produced in the reaction ^{58}Ni + ^{92}Mo. *Z. Phys. A* **305**, 125–130 (1982).
26. Gillitzer, A., Faestermann, T., Hartel, K., Kienle, P. & Nolte, E. Groundstate proton radioactivity of nuclei in the tin region. *Z. Phys. A* **326**, 107–119 (1987).
27. Woods, P. J. & Davids, C. N. Nuclei beyond the proton drip-line. *Annu. Rev. Nucl. Part. Sci.* **47**, 541–590 (1997).
28. Page, R. D. et al. Evidence for the alpha decay of ^{108}I. *Z. Phys. A* **338**, 295–301 (1991).
29. Auranen, K. et al. Proton decay of ^{108}I and its significance for the termination of the astrophysical *rp*-process. *Phys. Lett. B* **792**, 187–192 (2019).
30. Page, R. D. et al. Decays of odd-odd N-Z=2 nuclei above ^{100}Sn: The observation of proton radioactivity from ^{112}Cs. *Phys. Rev. Lett.* **72**, 1798 (1994).
31. Patial, M., Arumugam, P., Jain, A. K., Maglione, E. & Ferreira, L. S. Nonadiabatic quasiparticle approach for deformed odd-odd nuclei and the proton emitter ^{130}Eu. *Phys. Rev. C* **88**, 054302 (2013).
32. Soramel, F. et al. New strongly deformed proton emitter: ^{117}La. *Phys. Rev. C* **63**, 031304(R) (2001).
33. Mahmud, H. et al. Proton radioactivity of ^{117}La. *Phys. Rev. C* **64**, 031303(R) (2001).
34. Liu, Z. et al. Structure of the proton emitter ^{117}La studied by proton and γ-ray spectroscopy. *Phys. Lett. B* **702**, 24–27 (2011).
35. Schmidt, K. H. et al. Some remarks on the error analysis in the case of poor statistics. *Z. Phys. A* **316**, 19–26 (1984).
36. Möller, P., Sierk, A. J., Ichikawa, T. & Sagawa, H. Nuclear ground-state masses and deformations: FRDM(2012). *At. Data Nucl. Data Tables* **109–110**, 1–204 (2016).
37. Nilsson, S. G. Binding states of individual nucleons in strongly deformed nuclei. *Dan. Mat. Fys. Medd.* **29**, 16 (1955).
38. Liu, H. L., Xu, F. R., Xu, S. W., Wyss, R. & Walker, P. M. High-spin isomeric structures in exotic odd-odd nuclei: exploration of the proton drip line and beyond. *Phys. Rev. C* **76**, 034313 (2007).
39. Jain, A. K. et al. Atlas of nuclear isomers. *Nucl. Data Sheets* **128**, 1–130 (2015).
40. Zheng, K. K. et al. Complete set of proton excitations in ^{119}Cs. *Phys. Rev. C* **104**, 044305 (2021).
41. Cederwall, B. et al. Neutron and proton $h_{11/2}$ alignment effects in ^{121}La. *Z. Phys. A* **338**, 463–464 (1991).
42. Maglione, E., Ferreira, L. S. & Liotta, R. Proton emission from deformed nuclei. *Phys. Rev. C* **59**, R589 (1999).
43. Barmore, B., Kruppa, A. T., Nazarewicz, W. & Vertse, T. Theoretical description of deformed proton emitters: nonadiabatic coupled-channel method. *Phys. Rev. C* **62**, 054315 (2000).
44. Esbensen, H. & Davids, C. N. Coupled-channels treatment of deformed proton emitters. *Phys. Rev. C* **63**, 014315 (2001).
45. Lopes, M. C., Maglione, E. & Ferreira, L. S. Evidence for partial rotation alignment in proton emitting ^{121}Pr. *Phys. Lett. B* **673**, 15–18 (2009).
46. Qi, C., Xu, F. R., Liotta, R. J. & Wyss, R. Universal decay law in charged-particle emission and exotic cluster radioactivity. *Phys. Rev. Lett.* **103**, 072501 (2009).
47. Delion, D. S. *Theory of Particle and Cluster Emission* (Springer-Verlag, Berlin, 2010).
48. Delion, D. S., Liotta, R. J. & Wyss, R. Systematics of proton emission. *Phys. Rev. Lett.* **96**, 072501 (2006).
49. Doherty, D. T. et al. Solving the puzzles of the decay of the heaviest known proton-emitting nucleus ^{185}Bi. *Phys. Rev. Lett.* **127**, 202501 (2021).
50. Blank, B. & Borge, M. J. G. Nuclear structure at the proton drip line: Advances with nuclear decay studies. *Prog. Part. Nucl. Phys.* **60**, 403–483 (2008).
51. Darby, I. G. et al. Precision measurements of proton emission from the ground states of ^{156}Ta and ^{160}Re. *Phys. Rev. C* **83**, 064320 (2011).
52. Möller, P., Mumpower, M. R., Kawano, T. & Myers, W. D. Nuclear properties for astrophysical and radioactive-ion-beam applications (II). *At. Data Nucl. Data Tables* **125**, 1–192 (2019).
53. Qi, C., Delion, D. S., Liotta, R. J. & Wyss, R. Effects of formation properties in one-proton radioactivity. *Phys. Rev. C* **85**, 011303(R) (2012).
54. Qi, C., Liotta, R. & Wyss, R. Recent developments in radioactive charged-particle emissions and related phenomena. *Prog. Part. Nucl. Phys.* **105**, 214–251 (2019).
55. Maglione, E., Ferreira, L. S. & Liotta, R. Nucleon decay from deformed nuclei. *Phys. Rev. Lett.* **81**, 538 (1998).
56. Rykaczewski, K. et al. Proton emitters ^{140}Ho and ^{141}Ho: Probing the structure of unbound Nilsson orbitals. *Phys. Rev. C* **60**, 011301 (1999).
57. Koura, H. et al. Nuclidic mass formula on a spherical basis with an improved even-odd term. *Prog. Theor. Phys.* **113**, 305–325 (2005).
58. Macchiavelli, A. O. et al. Is there np pairing in $N = Z$ nuclei? *Phys. Rev. C* **61**, 041303(R) (2000).
59. Pastore, K., Barranco, F., Broglia, R. A. & Vigezzi, E. Microscopic calculation and local approximation of the spatial dependence of the pairing field with bare and induced interactions. *Phys. Rev. C* **72**, 024315 (2008).
60. Ferreira, L. S., Maglione, E. & Ring, P. Covariant density functional theory for decay of deformed proton emitters: a self-consistent approach. *Phys. Lett. B* **753**, 237 (2016).
61. Uusitalo, J., Sarén, J., Partanen, J. & Hilton, J. Mass analyzing recoil apparatus, MARA. *Acta Physica Polonica B* **50**, 319–327 (2019).
62. Sarén, J. et al. The new vacuum-mode recoil separator MARA at JYFL. *Nucl. Instr. Meth. Phys. Res. A* **266**, 4196–4200 (2008).
63. Lazarus, I. et al. The GREAT triggerless total data readout method. *IEEE Trans. Nucl. Sci.* **48**, 567–569 (2001).
64. Rahkila, P. Grain - A Java data analysis system for Total Data Readout. *Nucl. Instrum. Methods Phys. Res. Sect. A* **595**, 637–642 (2008).
65. Heine, F. et al. Proton and alpha radioactivity of very neutron deficient Te, I, Xe and Cs isotopes, studied after electrostatic separation. *Z. Phys. A* **340**, 225–226 (1991).
66. Krane, K. S. *Introductory Nuclear Physics* (Wiley, 1987).
67. Schmidt, K. H. A new test for random events of an exponential distribution. *Eur. Phys. J. A* **8**, 141–145 (2000).

68. Huang, K. N. et al. Neutral-atom electron binding energies from relaxed-orbital relativistic Hartree-Fock-Slater calculations $2 \le Z \le 106$. *Atomic Data and Nuclear Data Tables* **8**, 243–291 (1976).
69. Becchetti Jr, F. D. & Greenlees, G. W. Nucleon-nucleus optical-model parameters, $A > 40$, $E < 50$ MeV. *Phys. Rev.* **182**, 1190 (1969).

Acknowledgements

This work was supported by the Swedish Research Council under Grant No. 2019-04880; the United Kingdom Science and Technology Facilities Council (STFC) under Grants Nos. ST/P003885/1, ST/V001035/1, ST/P004598/1, and ST/V001027/1; the EU 7th Framework Programme, Integrating Activities Transnational Access, project No.262010 ENSAR; and the Academy of Finland under the Finnish Centre of Excellence Programme (Nuclear and Accelerator Based Physics Programme at JYFL). We thank the JYFL Accelerator laboratory staff for excellent operation of the K130 cyclotron and D. Delion, R. Liotta, N. Sandulescu, and C. Qi for fruitful discussions.

Author contributions

B.C. and J.U. prepared the proposal for the experiment. J.S., J.U., M.S., and J.O. set up the instrumentation. W.Z., B.C., Ö.A., X.L., A.E., A.N., H. Badran, H. Boston, M.D., U.F., T.G., P.T.G., S.G., J. Heery, J. Hilton, D.J., R.J., S.J., M.L., O.N., J.O., R.D.P., J. Pakarinen, J. Partanen, E.S.P., C.P., P. Rahkila, P. Ruotsalainen, M.S., J.S., S.S., H.T., J.U., and R.W. monitored the detector, data acquisition and beam systems. W.Z. and B.C. carried out the data analysis and interpretation of the data, and prepared the manuscript. All authors read the manuscript and took part in discussing the results and their implications.

Funding

Open access funding provided by Royal Institute of Technology.

Competing interests

The authors declare no competing interests.

Additional information

Supplementary information The online version contains supplementary material available at https://doi.org/10.1038/s42005-022-01069-w.

Correspondence and requests for materials should be addressed to Wei Zhang or Bo Cederwall.

Peer review information *Communications Physics* thanks the anonymous reviewers for their contribution to the peer review of this work. Peer reviewer reports are available.

Reprints and permission information is available at http://www.nature.com/reprints

Publisher's note Springer Nature remains neutral with regard to jurisdictional claims in published maps and institutional affiliations.